

## Pharmacologic Inhibition of Cyclin-Dependent Kinases 4 and 6 Arrests the Growth of Glioblastoma Multiforme Intracranial Xenografts

Karine Michaud<sup>1</sup>, David A. Solomon<sup>2</sup>, Eric Oermann<sup>2</sup>, Jung-Sik Kim<sup>2</sup>, Wei-Zhu Zhong<sup>3</sup>, Michael D. Prados<sup>1</sup>, Tomoko Ozawa<sup>1</sup>, C. David James<sup>1</sup>, and Todd Waldman<sup>2</sup>

### Abstract

Activation of cyclin-dependent kinases 4 and 6 (cdk4/6) occurs in the majority of glioblastoma multiforme (GBM) tumors, and represents a promising molecular target for the development of small molecule inhibitors. In the current study, we investigated the molecular determinants and *in vivo* response of diverse GBM cell lines and xenografts to PD-0332991, a cdk4/6-specific inhibitor. *In vitro* testing of PD-0332991 against a panel of GBM cell lines revealed a potent G<sub>1</sub> cell cycle arrest and induction of senescence in each of 16 retinoblastoma protein (Rb)-proficient cell lines regardless of other genetic lesions, whereas 5 cell lines with homozygous inactivation of Rb were completely resistant to treatment. Short hairpin RNA depletion of Rb expression conferred resistance of GBM cells to PD-0332991, further demonstrating a requirement of Rb for sensitivity to cdk4/6 inhibition. PD-0332991 was found to efficiently cross the blood-brain barrier and proved highly effective in suppressing the growth of intracranial GBM xenograft tumors, including those that had recurred after initial therapy with temozolomide. Remarkably, no mice receiving PD-0332991 died as a result of disease progression while on therapy. Additionally, the combination of PD-0332991 and radiation therapy resulted in significantly increased survival benefit compared with either therapy alone. In total, our results support clinical trial evaluation of PD-0332991 against newly diagnosed as well as recurrent GBM, and indicate that Rb status is the primary determinant of potential benefit from this therapy. *Cancer Res*; 70(8); 3228–38. ©2010 AACR.

### Introduction

Deregulation of the cyclin-dependent kinases 4 and 6 (cdk4/6)-cyclin D-INK4-retinoblastoma protein (Rb) signaling pathway is among the most common aberrations found in human cancer (1). In the case of glioblastoma multiforme (GBM), this pathway is most commonly altered by homozygous deletion of *CDKN2A/B*, and less commonly by deletion/mutation of *CDKN2C* and *RBI*, or genomic amplification of

*CDK4*, *CDK6*, and individual D-type cyclins (2–8). Recent molecular profiling of GBM has further highlighted the critical role of cdk4/6 activation in the pathogenesis of this devastating tumor (9, 10).

Despite the ubiquitous nature of cdk4/6 activation in human cancer, surprisingly little work has been reported describing efforts to target activated cdk4/6 with pharmacologic inhibitors. This is due to the difficulty of identifying inhibitors specific to cdk4/6, and also because cdk inhibition is predicted to be cytostatic (not cytotoxic), and therefore of uncertain therapeutic utility (11).

PD-0332991 is a recently developed cdk4/6-specific inhibitor. Initial reports detailed the synthesis of this pyridopyrimidine derivative, showed its *in vitro* specificity against cdk4/6, and documented its potent antiproliferative activity against Rb-proficient subcutaneous human tumor xenografts (12, 13). A large phase I study of this compound is ongoing and has already shown clinical efficacy against otherwise untreatable teratomas (14). Additional xenograft studies modeling disseminated multiple myeloma (15) and breast carcinoma (16) helped to motivate recently initiated phase I/II clinical trials testing PD-0332991 against these cancers (<http://www.clinicaltrials.gov>).

Given its effectiveness in a variety of tumor types and its specificity for activated cdk4/6, we hypothesized that PD-0332991 could be useful in the treatment of GBM. To evaluate this, PD-0332991 was initially tested *in vitro* against a panel of

**Authors' Affiliations:** <sup>1</sup>Department of Neurological Surgery, Helen Diller Comprehensive Cancer Center, University of California San Francisco, San Francisco, California; <sup>2</sup>Department of Oncology, Lombardi Comprehensive Cancer Center, Georgetown University School of Medicine, Washington, District of Columbia; and <sup>3</sup>Department of Pharmacokinetics, Dynamics and Metabolism, Pfizer Global Research and Development, La Jolla, California

**Note:** Supplementary data for this article are available at Cancer Research Online (<http://cancerres.aacrjournals.org/>).

K. Michaud and D.A. Solomon contributed equally to this work.

**Corresponding Authors:** Todd Waldman, Department of Oncology, Lombardi Comprehensive Cancer Center, E304 Research Building, 3970 Reservoir Road, Washington, DC 20057. Phone: 202-687-1340; Fax: 202-687-7505; E-mail: [waldmant@georgetown.edu](mailto:waldmant@georgetown.edu) and C. David James, Department of Neurosurgery, Brain Tumor Research Center, 1450 3rd Street, Room HD283 Northwest, University of California, San Francisco, San Francisco, CA 94143-0520. Phone: 415-476-5876; E-mail: [david.james@ucsf.edu](mailto:david.james@ucsf.edu).

doi: 10.1158/0008-5472.CAN-09-4559

©2010 American Association for Cancer Research.

21 human GBM cell lines of defined genetic backgrounds. Next, its activity was assayed *in vivo* against three different GBM intracranial xenografts using a luciferase reporter to allow longitudinal monitoring of tumor growth and response to therapy. Finally, PD-0332991 was tested in combination with ionizing radiation against intracranial xenografts, as well as in tumors that had recurred following initial therapy with temozolomide, an alkylating agent routinely used in upfront treatment of GBM (17). Our findings show that PD-0332991 crosses the blood-brain barrier and works effectively both as a single agent and in combination with radiation to suppress the growth of all Rb-proficient GBM cells and tumors tested.

## Materials and Methods

**GBM cell lines and xenografts.** A panel of 21 GBM cell lines was obtained directly from the American Type Culture Collection (U87MG, U138MG, M059J, Hs683, H4, A172, LN18, LN229, CCF-STTG1, T98G, and DBTRG-05MG), DSMZ (8MGBA, 42MGBA, DKMG, GAMG, GMS10, LN405, and SNB19), and the Japan Health Sciences Foundation Health Science Research Resources Bank (AM38, NMC-G1, and KG-1-C). These repositories authenticate all human cell lines prior to accession by DNA fingerprinting, and independent evidence of authenticity is also provided by cytogenetic and immunophenotypic tests. All experiments were performed on cell lines that had been passaged for <6 mo after receipt. Cell line SF767 was established from a GBM at the University of California, San Francisco Brain Tumor Research Center, and has been previously genotyped for *CDKN2A*, *TP53*, and *PTEN* status (18). All cell lines were grown in DMEM + 10% fetal bovine serum at 37°C in 5% CO<sub>2</sub>. GBM 39 is a human GBM primary xenograft maintained as a subcutaneous heterotransplant in athymic mice, as previously described (19).

**Western blot.** Total cell lysate was collected from asynchronously proliferating cells in radioimmunoprecipitation assay buffer, resolved by SDS-PAGE, and then immunoblotted using standard techniques. Primary antibodies used were obtained from Santa Cruz Biotechnology (Mdm2, clone SMP14), Cell Signaling (cyclin D1, clone DCS6; cyclin D3, clone DCS22; cdk4, clone DCS156; cdk6, clone DCS83; p18INK4c, clone DCS118; p21WAF1/CIP1, clone DCS60; p14ARF, clone 4C6/4; Rb, clone 4H1), BD PharMingen (p16INK4a, no. 554079), NeoMarkers ( $\alpha$ -tubulin, Ab-1 clone DM1A; EGFR, Ab-12), Calbiochem (p53, Ab-6 clone DO-1), and Cascade Bioscience (PTEN, clone 6H2.1).

**Flow cytometry.** Cells were pulsed with 10  $\mu$ M of bromodeoxyuridine (BrdUrd) for 1 h, trypsinized, and then centrifuged. Cells were fixed and stained using the BrdU Flow Kit (PharMingen), counterstained with propidium iodide, and analyzed by flow cytometry in a BD FACSort instrument using FCS Express v.3 software (DeNovo Software).

**$\beta$ -Galactosidase staining.** Cells grown on coverslips were stained with the Senescence  $\beta$ -Galactosidase Staining Kit (Cell Signaling) as described by the manufacturer.

**Microscopy.** Imaging was performed on an Olympus BX61 light microscope with Plan-Apochromat objectives.

**Rb knockdown.** Five unique short hairpin RNAs (shRNA) to the Rb1 mRNA in the pLKO.1-Puro lentiviral expression vector were obtained from Open Biosystems. To make the virus, empty pLKO.1-Puro or each of these five shRNA clones were cotransfected into 293T cells with pVSV-G (Addgene) and pHR'-CMV-8.2 $\Delta$ R (Addgene) helper plasmids using Fugene 6 (Roche). Virus-containing conditioned medium was harvested 48 h after transfection, filtered, and used to infect recipient cells in the presence of 8  $\mu$ g/mL of polybrene. Infected cells were selected with 2  $\mu$ g/mL of puromycin until all mock-infected cells were dead and then maintained in 0.2  $\mu$ g/mL of puromycin.

**Generation and therapy of mice with intracranial GBM xenograft tumors.** All intracranial therapy response experiments involved the use of 5- to 6-week-old female athymic mice (*nu/nu* genotype, BALB/c background; Simonsen Laboratories). Animals were housed and fed under aseptic conditions, and all animal research was approved by The University of California, San Francisco Institutional Animal Care and Use Committee. Procedures used for intracranial tumor establishment, including monitoring of tumor growth and response to therapy by bioluminescence imaging, have previously been described (20). Treatments for the experiments reported here were as follows: oral administration of vehicle only for control groups [50 mmol/L sodium lactate (pH 4), for PD-0332991, and/or OraPlus for temozolomide], oral administration of PD-0332991 (Pfizer) at 150 mg/kg/d, clinical grade temozolomide (Schering-Plough) at 10 mg/kg/d, and radiation at 2 Gy/d from a Cesium-137 source (J.L. Shepherd & Associates).

**Brain tumor analysis.** PD-0332991 concentrations in mouse brain or brain tumor were determined using a liquid chromatography-tandem mass spectrometry (LC-MS/MS) method following liquid-liquid extraction. Brain or brain tumor samples were homogenized with purified water at 1:4 dilution (w/v). A 100  $\mu$ L aliquot of the homogenate was used for liquid-liquid extraction with the addition of 100  $\mu$ L of potassium bicarbonate buffer, 10  $\mu$ L of the stable labeled internal standard, and 0.4 mL of methyl tert-butyl ether. Following centrifugation, the organic layer was evaporated to dryness and reconstituted in 100  $\mu$ L of methanol for LC-MS/MS analysis. The LC system (Shimadzu) was coupled to an MDS Sciex API 4000 triple quadrupole mass spectrometer, and operated in the positive ionization mode using a multiple reaction source. PD-0332991 and internal standard were monitored using specific precursor ion  $\rightarrow$  product ion transitions of  $m/z$  448  $\rightarrow$  380 and  $m/z$  451  $\rightarrow$  383, respectively. The final concentration of PD-0332991 was normalized based on the weight of mouse brain or brain tumor collected.

## Results

**Ubiquitous genetic lesions of the *cdk4/6*-cyclin *D-INK4-Rb* signaling pathway in GBM cell lines.** Copy number and sequencing data from our previous analyses (7, 21, 22) and from the Cancer Genome Project of the Wellcome Trust Sanger Institute (<http://www.sanger.ac.uk/genetics/CGP>) were analyzed to identify the genetic status of the major

**Table 1.** Genetic lesions of the cdk4/6-cyclin D-INK4-Rb signaling pathway and *in vitro* sensitivity to PD-0332991 for a panel of 21 GBM cell lines

Cell line	Sensitivity to 1 $\mu\text{mol/L}$ of PD-0332991*	Genetic lesions present in cells <sup>†</sup>							
		RB1	CDKN2A/B	CDKN2C	CDK4 <sup>‡</sup>	CDK6 <sup>‡</sup>	CCND1 <sup>‡</sup>	CCND2 <sup>‡</sup>	CCND3 <sup>‡</sup>
8MGBA	–	HD							
42MGBA	–	No protein <sup>‡</sup>	HD						
A172	+++		HD						
AM-38	++		HD						
CCF-STTG1	+++					AMP			AMP
DBTRG-05MG	+++		HD						
DKMG	+++		HD						
GAMG	+		HD						
GMS10	–	MUT (nonsense)							
H4	+		HD						
Hs683	+++	‡	HD						
KG-1-C	+++	‡	HD						
LN18	+	‡	HD						
LN229	+++	‡	HD	HD					
LN405	–	MUT (nonsense)							
M059J	–	MUT (splice site)							
NMC-G1	+++		HD						
SNB19	+++		HD	HD					
T98G	+		HD	HD					
U138MG	+++		HD						
U87MG	+++		HD	HD					
Total events	16	5	16	4	0	1	0	0	1
Frequency	76%	24%	76%	19%	0%	5%	0%	0%	5%

Abbreviations: HD, homozygous deletion; MUT, homozygous mutation; AMP, genomic amplification.

\*A panel of 21 GBM cell lines was grown *in vitro* in the presence of vehicle or 1  $\mu\text{mol/L}$  of PD-0332991 for 48 h, pulsed with BrdUrd for 1 h, then fixed and stained with propidium iodide and FITC-conjugated BrdUrd antibody for flow cytometry analysis (see Supplementary Fig. S2). A sensitivity score of +++ was assigned to cells with >95% reduction in BrdUrd incorporation after treatment with 1  $\mu\text{mol/L}$  of PD-0332991 compared with vehicle; ++ for 75% to 95% reduction; + for 10% to 75% reduction; and – for <10% reduction.

<sup>†</sup>Genetic data are derived from exonic sequencing and Affymetrix 250K SNP arrays performed by Solomon and colleagues (7, 21, 22) and from Affymetrix 6.0 SNP arrays and the COSMIC database of the Cancer Genome Project of the Wellcome Trust Sanger Institute (<http://www.sanger.ac.uk/genetics/CGP/>).

<sup>‡</sup>Mutation status of gene not determined.

known GBM oncogenes and tumor suppressor genes in a panel of 21 GBM cell lines. This analysis showed genetic lesions in at least one component of the cdk4/6-cyclin D-INK4-Rb signaling pathway in each cell line, without exception (Table 1). Fifteen of the cell lines have homozygous deletions of *CDKN2A* and *CDKN2B*, five have homozygous deletions or mutations of *RB1* (resulting in a lack of detectable Rb protein), four have homozygous deletions of *CDKN2C*, and one (CCF-STTG1) harbors amplifications of both *CDK6* and *CCND3*, with high levels of expression of corresponding encoded proteins (Table 1; Supplementary Fig. S1). Lesions of *CDKN2A/B*, *RB1*, and *CDK6/CCND3* were mutually exclusive in these 21 cell lines, except for 42MGBA cells, which harbor homozygous deletion of *CDKN2A/B* and express no detectable

Rb protein. In contrast, homozygous deletion of *CDKN2C* occurred exclusively in cell lines also harboring homozygous deletions of *CDKN2A/B*. A number of additional genetic lesions in other signaling pathways were identified among the cell lines, including *PTEN* deletion and mutation, *TP53* mutation, *BRAF* mutation, *EGFR* rearrangement, and *MDM2* amplification (Supplementary Table S1). However, no concordance was detected between any of these other genetic lesions and lesions of cdk4/6-cyclin D-INK4-Rb signaling pathway genes.

**PD-0332991 induces cell cycle arrest and senescence of Rb-proficient GBM cells.** Twenty-one GBM cell lines were cultured *in vitro* in the presence of either 1  $\mu\text{mol/L}$  of PD-0332991 or vehicle alone. At 48 hours posttreatment, cell

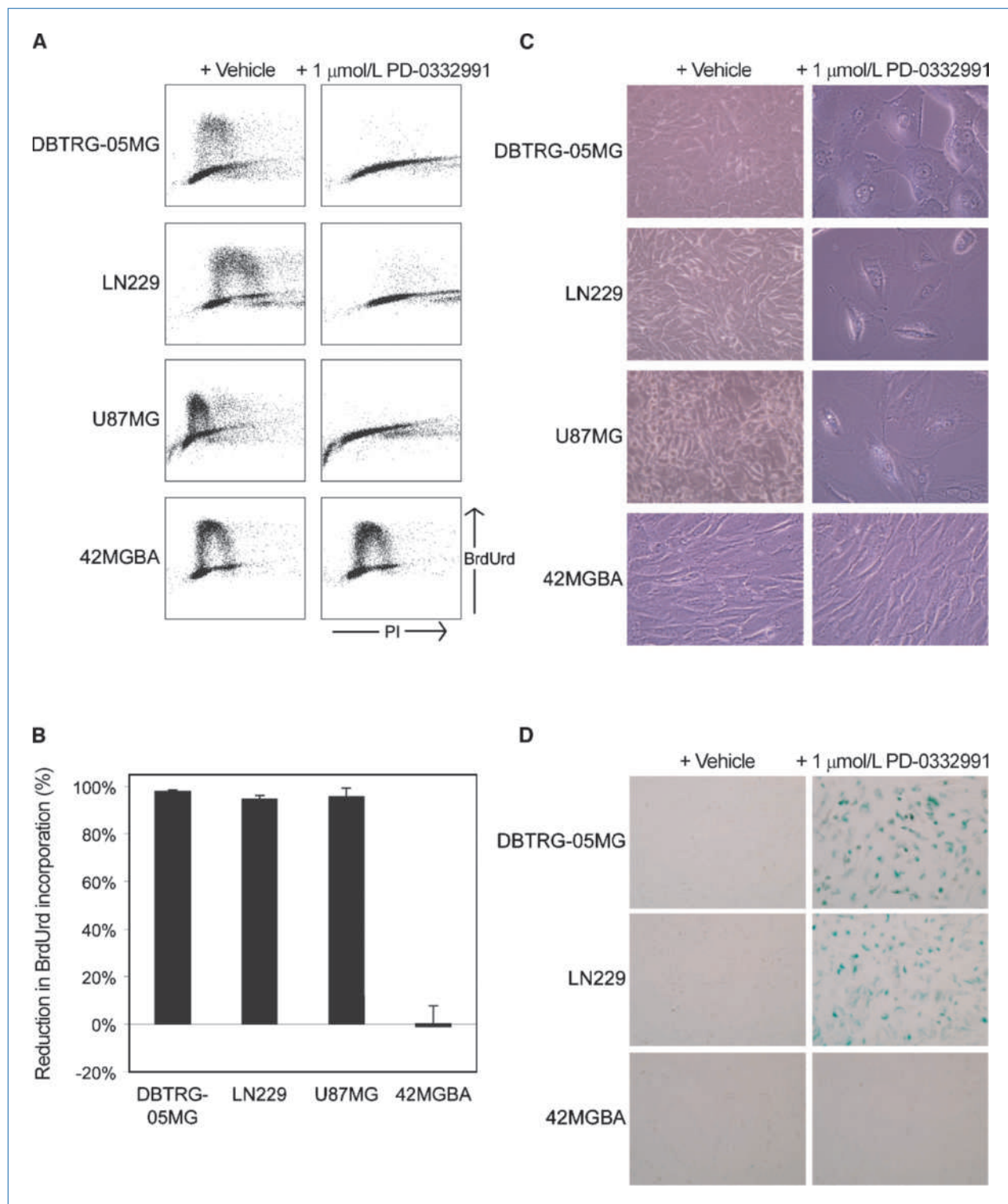
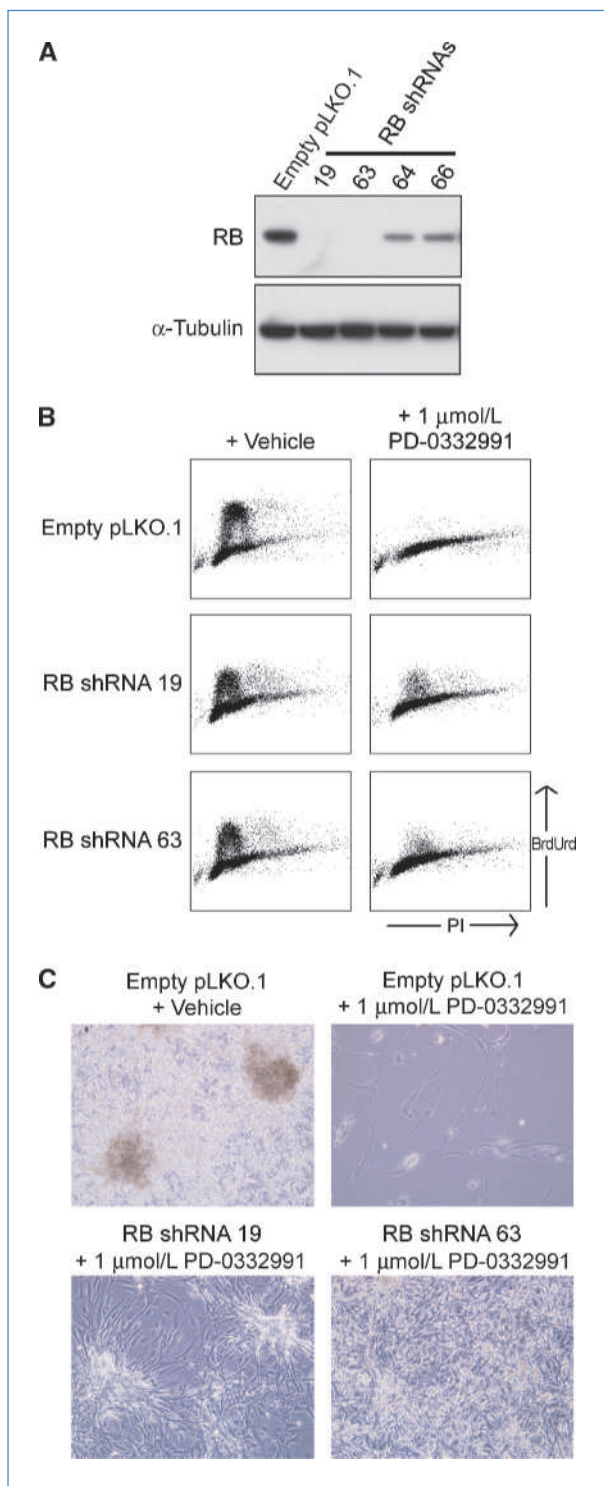


**Figure 1.** PD-0332991 induces cell cycle arrest and senescence of GBM cells dependent on Rb status. **A**, flow cytometry analysis of three Rb-proficient GBM cell lines (DBTRG-05MG, LN229, and U87MG) and one Rb-deficient cell line (42MGBA) following culture in the presence of vehicle or 1  $\mu\text{mol/L}$  of PD-0332991 for 48 h and then pulsed with BrdUrd for 1 h. Cell cycle distribution plots of BrdUrd versus propidium iodide (PI) intensity. **B**, quantification of reduction in S phase cells in **A**. **C**, photomicrographs of the Rb-proficient cell lines after culture in the presence of 1  $\mu\text{mol/L}$  of PD-0332991 for 7 d reveal growth inhibition and morphologic changes resembling cellular senescence, whereas the Rb-deficient cell line (42MGBA) shows no growth inhibition or morphologic changes. **D**, staining for senescence-associated  $\beta$ -galactosidase activity in two Rb-proficient cell lines and one Rb-deficient cell line after culture in the presence of vehicle or 1  $\mu\text{mol/L}$  of PD-0332991 for 2 wk.

cycle distribution was assessed by BrdUrd incorporation and flow cytometry analysis (Fig. 1A and B; Supplementary Fig. S2). In 16 of 21 cell lines, PD-0332991 treatment significantly inhibited BrdUrd incorporation and resulted in an increased fraction of cells in G<sub>1</sub> phase of the cell cycle



compared with vehicle alone (Table 1). Although some cell lines displayed a >95% reduction in BrdUrd incorporation after treatment with 1 μmol/L of PD-0332991 for 48 hours (e.g., A172, CCF-STTG1, DBTRG-05MG, DKMG, Hs683, KG-1-C, NMC-G1, SNB19, and U87MG), others displayed a more intermediate response (e.g., AM38, GAMG, H4, and LN18). Of note, 5 of 21 of these cell lines displayed no difference in cell cycle distribution between treatment with vehicle or 1 μmol/L of PD-0332991 (8MGBA, 42MGBA, GMS10, LN405, and M059J). Remarkably, each of the five resistant cell lines harbors homozygous deletion or mutation of the *RB1* gene that results in the absence of detectable Rb protein (see Supplementary Fig. S1).

To further explore the differential sensitivity of GBM cell lines to PD-0332991, the 21 cell lines were next cultured in the presence of 0, 1, 2, or 10 μmol/L of PD-0332991, and cell cycle distribution was again assessed at 48 hours posttreatment (Supplementary Fig. S3). Cells that initially displayed >95% reduction in BrdUrd incorporation at 1 μmol/L showed similar inhibition at doses of 2 and 10 μmol/L PD-0332991, and without evidence of apoptosis or cytotoxicity (i.e., floating cell debris or sub-G<sub>1</sub> DNA content) at any dose (data not shown). Importantly, Rb-proficient cells that displayed intermediate reductions in BrdUrd incorporation at 1 μmol/L PD-0332991 displayed increased reductions when incubated with 2 and 10 μmol/L of PD-0332991. For example, GAMG cells displayed a 53% reduction in BrdUrd incorporation at 1 μmol/L PD-0332991, but had 78% and 96% reductions at 2 and 10 μmol/L, respectively. In contrast, the five Rb-deficient cell lines displayed no reduction in BrdUrd incorporation or alterations in cell cycle distribution at any of the doses tested.

We next examined the effects of long-term culture in the presence of PD-0332991. Microscopic analysis of Rb-proficient GBM cells treated with 1 μmol/L of PD-0332991 for 7 days revealed not only sustained growth arrest, but also morphologic changes characteristic of cells that have exited the cell cycle and entered a senescent-like state (i.e., large and flat; Fig. 1C). Senescence-associated β-galactosidase activity was evident in Rb-proficient GBM cells after 14 days of treatment with PD-0332991 (Fig. 1D). However, Rb-deficient cells did not display these morphologic and senescent-like changes (Fig. 1C and D). Together, these findings indicate that PD-0332991 potently induces G<sub>1</sub> cell cycle arrest of GBM cells at doses of <1 to 10 μmol/L, and that sustained treatment induces cellular senescence in Rb-proficient cells.

**Stable depletion of Rb expression alleviates the growth arrest induced by PD-0332991.** To unequivocally determine

**Figure 2.** Depletion of Rb expression alleviates growth arrest induced by PD-0332991. A, five unique shRNAs to RB1 were transduced into U87MG cells, and total protein from stably expressing pooled clones was resolved by SDS-PAGE and immunoblotted with a Rb antibody. Clones 19 and 63 show >99% knockdown of Rb expression relative to the empty pLKO.1-infected clone. B, flow cytometry analysis following a 1-h BrdUrd pulse of U87MG Rb shRNA clones 19 and 63 after 48 h of treatment with vehicle or 1 μmol/L of PD-0332991. C, photomicrographs of clones 19 and 63 following incubation with 1 μmol/L of PD-0332991 for 3 wk shows their failure to arrest and eventual growth to confluence in spite of sustained incubation with the cdk4/6 inhibitor.

if Rb status dictates the sensitivity of GBM cells to PD-0332991, U87MG cells were infected with lentiviruses expressing five unique shRNAs to *RBI*, and stably expressing pooled clones were generated by puromycin selection. Two of the clones (19 and 63) showed >99% knockdown of Rb expression relative to cells infected with the pLKO.1 vector alone (Fig. 2A). BrdUrd incorporation and flow cytometry analysis at 48 hours posttreatment revealed that Rb knockdown had substantially mitigated the cell cycle inhibitory effects of PD-0332991 in clones 19 and 63, relative to the empty vector pLKO.1 clone (Fig. 2B). Long-term culture of clones 19 and 63 with 1  $\mu$ mol/L of PD-0332991 showed their failure to arrest in the presence of drug, resulting in eventual growth to confluence (Fig. 2C), albeit at a slower rate than cells treated with vehicle alone.

**PD-0332991 suppresses the growth of GBM intracranial xenografts.** Next, we tested whether orally administered PD-0332991 could efficiently cross the blood-brain barrier and effectively suppress the growth of intracranial GBM tumors comprised of cells with known sensitivity *in vitro*. To do this, we established luciferase-modified U87MG xenografts in the brains of a series of athymic mice, with half receiving daily PD-0332991 by oral gavage, and the other half receiving vehicle only. Bioluminescence monitoring showed sustained anti-proliferative activity of PD-0332991 throughout the 4-week course of treatment (Fig. 3A, left), with tumor growth only evident upon completion of therapy. Consistent with these results, the survival of PD-0332991-treated mice was significantly extended relative to mice receiving vehicle only (Fig. 3A, right; Supplementary Table S2). Importantly, none of the mice receiving PD-0332991 succumbed to tumor-related death while on therapy. In contrast, intracranial xenografts derived from the Rb-deficient cell line SF767 were completely resistant to PD-0332991 treatment (Supplementary Fig. S4).

To provide formal proof that PD-0332991 crosses the blood-brain barrier, we dissected the brain of a mouse and measured the levels of PD-0332991 in the U87MG xenograft tumor, in surrounding normal brain, and in brain from contralateral hemisphere. Notably, LC-MS/MS analysis revealed the presence of PD-0332991 in all three intracranial tissues. Furthermore, the drug was present at a 25 $\times$  to 35 $\times$  higher concentration in tumor tissue than in normal tissue (Fig. 3B). Next, the brains from treated and untreated mice with intracranial U87MG tumors (matched with respect to their time of sacrifice) were formalin-fixed, embedded in paraffin, and sectioned for MIB-1 immunohistochemistry. Treatment with PD-0332991 led to an >8-fold reduction in MIB-1 index (Fig. 3C).

It is widely appreciated that established GBM cell lines do not recapitulate several aspects of GBM biology (e.g., *in vivo* invasiveness, the presence of genomic amplifications, gene expression profiles; refs. 19, 22–24). Therefore, we next tested the efficacy of PD-0332991 against a model system that has been shown to preserve patient tumor characteristics that are lost and/or suppressed with extended *in vitro* propagation—primary intracranial xenografts generated from surgically resected human tissue that have been directly implanted and serially passaged in nude mice (19). To do this, mice harboring primary intracranial xenografts of luciferase-modified GBM 39 (which harbors a homozygous deletion of the *CDKN2A/B* locus and is

Rb-proficient; ref. 25) were randomized to control and treatment groups at 25 days postinjection of tumor cells. Daily treatment with PD-0332991 resulted in sustained growth suppression (Fig. 3D, left), with significant survival benefit to treatment group mice (Fig. 3D, right; Supplementary Table S2).

**PD-0332991 combined with radiation therapy enhances the survival of mice with GBM intracranial xenografts.** Radiation has long been used as a standard of care for treating newly diagnosed GBM following surgical debulking of tumor (26), and investigational drugs for treating newly diagnosed GBM are likely to see use with radiotherapy. To assess combined effects of radiation and PD-0332991 therapy, we established U87MG intracranial tumors in the brains of athymic mice and randomized them to four treatment groups at day 13 postinjection of tumor cells: control (mock treated), radiotherapy only (2 Gy/d, days 13–17), PD-0332991 only (150 mg/kg/d, days 13–26), or combination therapy with radiation administered either concurrently or sequentially, with PD-0332991 and radiation combination regimens dosed identically to their corresponding monotherapy regimens. Both bioluminescence and survival analysis showed that antitumor activity was most pronounced for mice receiving combination therapy, either concurrent or sequential (Fig. 4A and B; Supplementary Table S2).

**PD-0332991 effectively suppresses the growth of recurrent GBM.** An additional clinical scenario that often provides a setting for initial testing of an investigational agent is the treatment of recurrent cancer. For modeling this situation, mice with intracranial U87MG tumors were treated with 10 mg/kg/d of temozolomide for 5 consecutive days, and subsequently monitored for initial antitumor activity of therapy, as well as for tumor regrowth from therapy (Fig. 5A). At the time of tumor regrowth, mice were randomized to four treatment groups: (a) no additional treatment, (b) repeat treatment with the same temozolomide regimen, (c) treatment with PD-0332991 at 150 mg/kg/d for 2 weeks, or (d) combined treatment with temozolomide and PD-0332991 administered concurrently at identical doses as the monotherapies. Both bioluminescence monitoring (Fig. 5B) and survival analysis (Fig. 5C; Supplementary Table S2) indicated that each therapy resulted in improved survival compared with no additional treatment. Furthermore, there was a trend favoring combination therapy with temozolomide and PD-0332991 as the most efficacious.

## Discussion

Frequent and perhaps obligatory genetic alteration affecting the cdk4/6-cyclin D-INK4-Rb growth-regulatory axis in GBM is well documented (refs. 2–8; Table 1 in the current report), and has been recently corroborated in two large-scale, multi-institutional genomic analyses of GBM (9, 10). The most common alteration of this pathway in GBM is homozygous deletion of *CDKN2A/B*, encoding p16<sup>INK4a</sup> and p15<sup>INK4b</sup>, which is present in >50% of tumors. Other alterations include amplification and overexpression of *CDK4* (15–20%) and homozygous deletion/mutation of *RBI* (~10%). Amplification of *CDK6* and individual D-type cyclins,

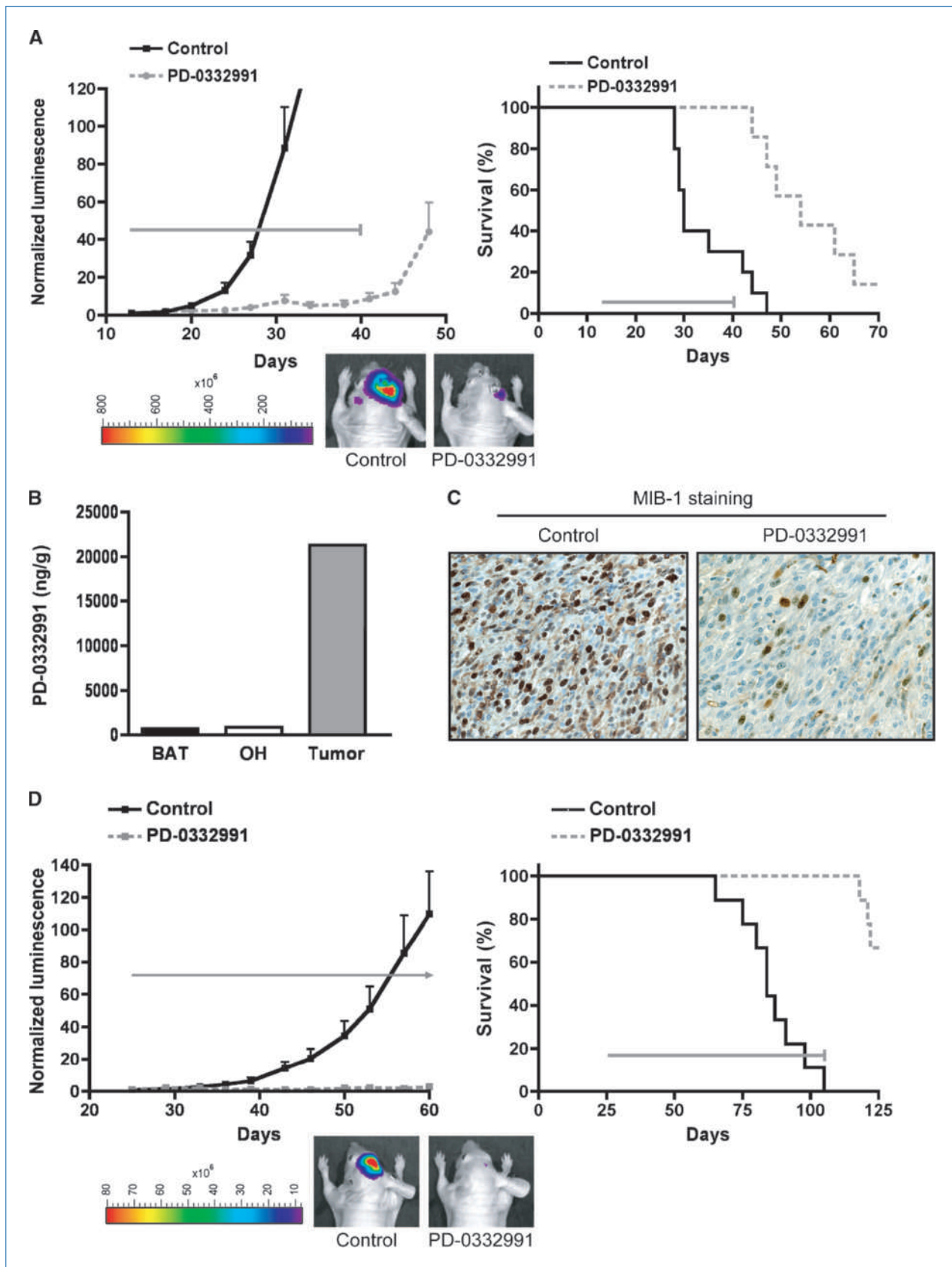
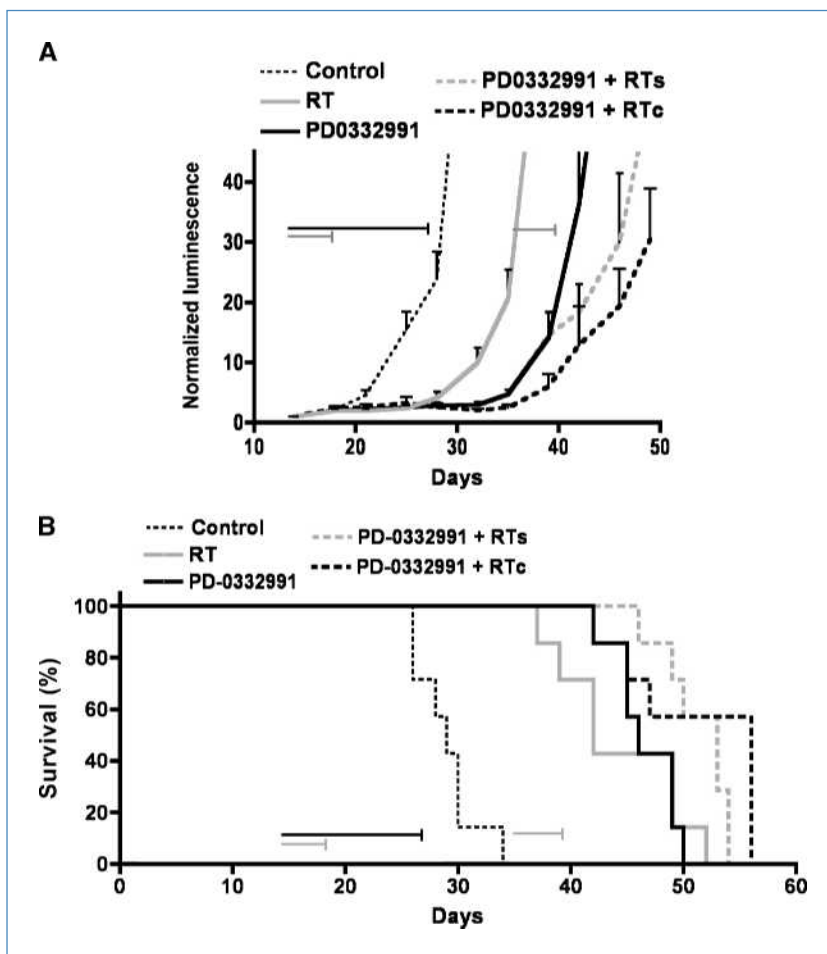


**Figure 4.** PD-0332991 combined with radiation therapy shows enhanced antitumor activity and extends survival. Luciferase-modified U87MG cells were injected into the brains of nude mice to establish intracranial tumors. Mice were randomized to four treatment groups: untreated (Control), radiation only (RT, 2 Gy/d for 5 d, horizontal gray lines), PD-0332991 only (150 mg/kg/d for 14 d, horizontal black lines), PD-0332991 and concurrent radiation (RTc), and PD-0332991 with subsequent radiation (RTs). A, bioluminescence monitoring was conducted once or twice weekly throughout the course of the experiment, with mean normalized values plotted for each treatment group. B, Kaplan-Meier survival plots demonstrating survival benefit from PD-0332991 and radiation combination therapy. See Supplementary Table S2 for statistical analysis of mean survival.



and homozygous deletion of *CDKN2C* encoding p18<sup>INK4c</sup> are less common. Of these alterations, only genetic inactivation of *RBI* itself is thought to render a tumor resistant to inhibition of cdk4/6. Because genetic inactivation of *RBI* occurs infrequently in GBM, a substantial majority of patients with GBM are predicted to be candidates for therapies targeting cdk4/6.

Several previous studies have tested the effects of kinase inhibitors against GBM (e.g., imatinib, erlotinib, and flavopir-

idol), both in a preclinical setting and in clinical trials without significant efficacy (27–29). Although some of these compounds promiscuously inhibit cdk (e.g., flavopiridol), none of the previously tested compounds display selectivity for cdk relative to other kinases that may or may not be activated in GBM. Our study for the first time tests a cdk-specific inhibitor in the treatment of GBM, demonstrating significant efficacy both *in vitro* and *in vivo* as a single agent and in combination with radiation therapy.

**Figure 3.** PD-0332991 crosses the blood-brain barrier and potently suppresses the growth of intracranial human GBM xenografts. U87MG cells (A–C) and primary xenograft GBM 39 (D) were modified to express luciferase and injected into the brains of nude mice to establish intracranial tumors. Mice were randomized to control (vehicle treated) and PD-0332991 treatment groups, with PD-0332991 administered daily by oral gavage at 150 mg/kg (4 wk for U87MG; 12 wk for GBM 39; see gray horizontal line and arrow in A and D, respectively). Mice were imaged once or twice weekly for bioluminescence intensity (see examples in A and D), with luminescence values of individual mice normalized to their corresponding luminescence at the start of therapy, and mean normalized values plotted (left, A and D). B, one mouse from the U87MG treatment group was euthanized and its brain was dissected for the isolation of pure tumor, brain adjacent to tumor (BAT), and normal tissue from the opposite hemisphere (OH). These specimens were analyzed by LC-MS/MS for determination of PD-0332991 content, which showed the dissemination of PD-0332991 into the brain and accumulation in tumor tissue. C, one mouse from the U87MG treatment group and one mouse from the control group were euthanized on the same day post-tumor cell injection, and their brains dissected, fixed, and embedded in paraffin. Immunohistochemistry with MIB-1 antibody revealed >8-fold reduction in MIB-1 index in the tumor from the PD-0332991-treated mouse relative to the control. A and D (right), Kaplan-Meier survival plots for the U87MG and GBM 39 experiments demonstrating significant survival benefit from PD-0332991 treatment ( $P < 0.001$  in each case). See Supplementary Table S2 for statistical analysis of mean survival.

PD-0332991 is an orally available pyridopyrimidine derivative that selectively inhibits cdk4/6 (12), leading to a reduction in Rb phosphorylation and subsequent cell cycle arrest. The *in vitro* and *in vivo* results presented here further emphasize that Rb is the primary determinant of sensitivity to cdk4/6 inhibition. This aspect of PD-0332991 efficacy should

be especially attractive with respect to clinical trial evaluation because there are excellent reagents and protocols established for immunohistochemical detection of Rb in paraffin-embedded tissues (14, 30).

Although Rb expression is clearly the primary determinant of tumor cell response to PD-0332991, variable growth inhibition

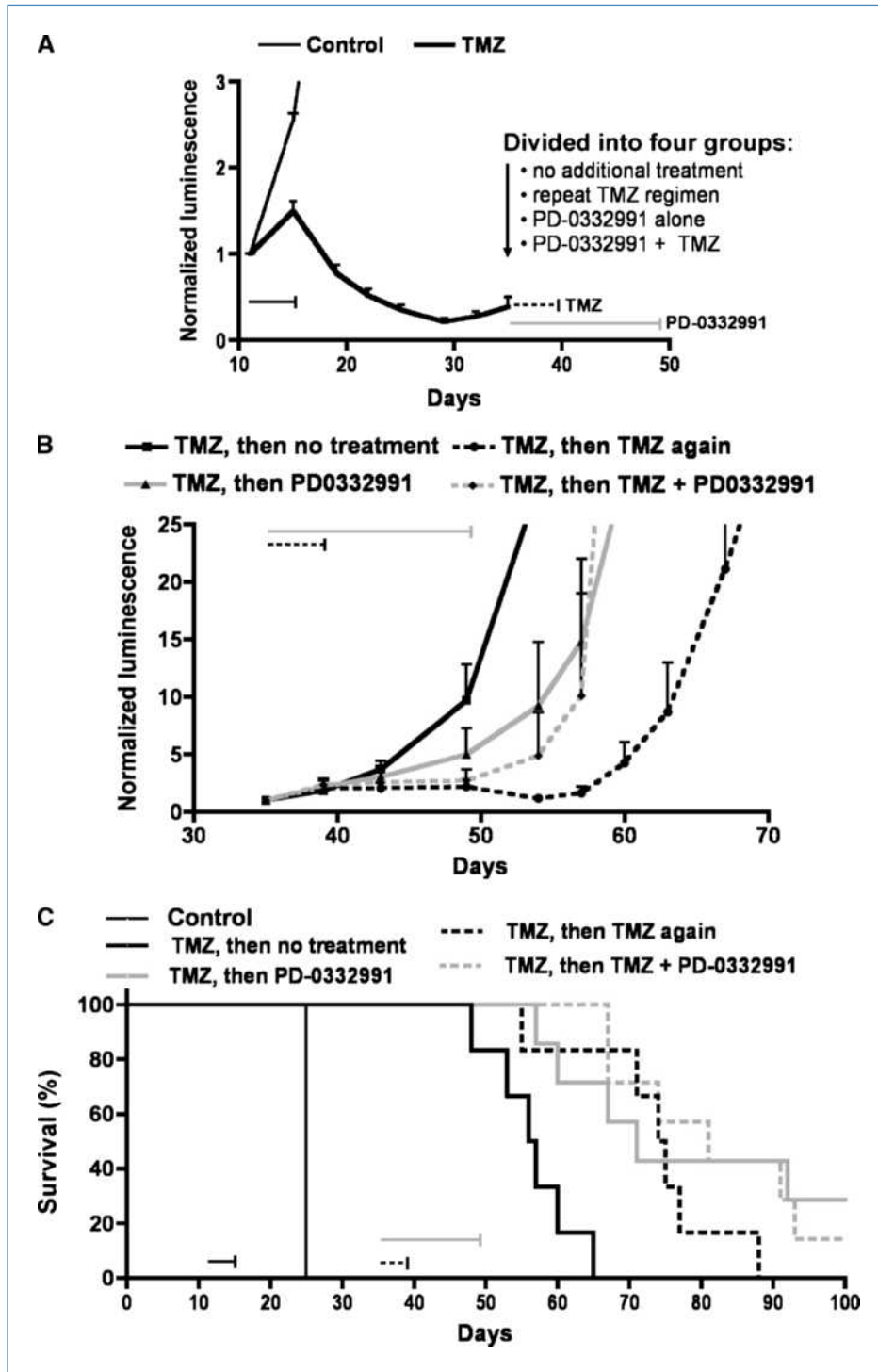


**Figure 5.** Evaluation of PD-0332991 activity against intracranial GBM xenografts that have recurred following initial treatment with temozolomide. A, luciferase-modified U87MG cells were injected into the brains of athymic mice. Mice with proliferating tumors were randomized into untreated (Control) and temozolomide-treated groups (TMZ, 10 mg/kg/d for 5 d). B, when successive mean normalized luminescence values indicated tumor recurrence of temozolomide-treated mice (day 35), these mice were randomized into four treatment groups: no additional treatment, repeat treatment with the same temozolomide regimen, treatment with PD-0332991 (150 mg/kg/d for 14 d), or combined temozolomide + PD-0332991 treatment, and then monitored for bioluminescent intensity once or twice weekly during therapy. C, Kaplan-Meier survival plots demonstrating significant survival benefit from PD-0332991 therapy of recurrent tumors. See Supplementary Table S2 for statistical analysis of mean survival.

among Rb-proficient cell lines (Table 1) suggests the existence of secondary factors that influence tumor cell sensitivity to PD-0332991, such as tumor CDK4/6 amplification versus CDKN2A homozygous deletion. For the cell lines examined here, the single case with CDK6 amplification (CCF-STTG1) showed substantial sensitivity to PD-0332991 (Table 1).

Analysis of GBM response to PD-0332991 *in vivo*, using three different GBM tumor cell sources for establishing intracranial tumors (Fig. 3), yielded results entirely consistent with the *in vitro* data. PD-0332991 arrested the growth of xenografts generated from U87MG cells and GBM 39 (both Rb-proficient) and led to significantly improved survival (Fig. 3). The growth-inhibitory effect of PD-0332991 was remarkably durable during the period of treatment.

Recent studies point to interest in investigating antitumor effects of PD-0332991 in combination with therapeutics that affect tumor properties other than cell cycling. For instance, it has been shown that PD-0332991, which by itself does not promote apoptotic response of cancer cells, markedly enhances myeloma cell killing by dexamethasone (15) as well as by bortezomib (31). Similarly, PD-0332991 has been shown to enhance breast cancer cell sensitivity to tamoxifen *in vitro* (32). Here, our bioluminescence and survival analysis of mice with intracranial U87MG tumors indicate that the antitumor activity of PD-0332991, when used with radiation either concurrently or sequentially, is superior to using either agent as a monotherapy (Fig. 4). These results, therefore, could help motivate clinical trial testing of PD-0332991 against newly diagnosed GBM, for which the use of radiotherapy is the standard of care.

Finally, treatment of intracranial GBM tumors that had regrown following initial therapy with temozolomide showed that PD-0332991 has activity against recurrent GBM (Fig. 5). These results additionally suggest a general approach for

preclinical animal model testing of therapies for patients with recurrent brain tumors, which is a mostly neglected area of neuro-oncology research.

In total, these findings provide strong support for evaluating the efficacy of PD-0332991 in treating patients with GBM. For future investigation, it will be interesting to examine combination therapies involving PD-0332991 with small molecule inhibitors targeting activated gene products in other GBM core pathways, such as erlotinib for inhibiting the epidermal growth factor receptor. Determination of the full range of applications of this cdk4/6 inhibitor will undoubtedly prove informative, and will hopefully lead to improved treatment for this devastating cancer.

### Disclosure of Potential Conflicts of Interest

No potential conflicts of interest were disclosed.

### Acknowledgments

We thank Karen Creswell and Annie Park for assistance with flow cytometry, Raquel Santos for assistance in conducting the intracranial xenograft therapy response experiments, Minerva Batugo for assistance with the LC-MS/MS analysis of brain tumor samples, and Michael Pishvaian and Erik Knudsen for helpful discussions.

### Grant Support

NIH grants CA097257 (K. Michaud, T. Ozawa, and C.D. James) and CA115699 (T. Waldman), and American Cancer Society grant RSG0619101MGO (T. Waldman). E. Oermann was supported by an American Brain Tumor Association Medical Student Summer Fellowship.

The costs of publication of this article were defrayed in part by the payment of page charges. This article must therefore be hereby marked *advertisement* in accordance with 18 U.S.C. Section 1734 solely to indicate this fact.

Received 01/06/2010; accepted 02/18/2010; published OnlineFirst 03/30/2010.

### References

- Malumbres M, Barbacid M. Cell cycle, CDKs and cancer: a changing paradigm. *Nat Rev Cancer* 2009;9:153–66.
- Jen J, Harper JW, Bigner SH, et al. Deletion of p16 and p15 genes in brain tumors. *Cancer Res* 1994;54:6353–8.
- He J, Allen JR, Collins VP, et al. CDK4 amplification is an alternative mechanism to p16 gene homozygous deletion in glioma cell lines. *Cancer Res* 1994;54:5804–7.
- He J, Olson JJ, James CD. Lack of p16INK4 or retinoblastoma protein (pRb), or amplification-associated overexpression of cdk4 is observed in distinct subsets of malignant glial tumors and cell lines. *Cancer Res* 1995;55:4833–6.
- Ichimura K, Schmidt EE, Goike HM, Collins VP. Human glioblastomas with no alterations of the CDKN2A (p16INK4A, MTS1) and CDK4 genes have frequent mutations of the retinoblastoma gene. *Oncogene* 1996;13:1065–72.
- Ueki K, Ono Y, Henson JW, Efrid JT, von Deimling A, Louis DN. CDKN2/p16 or RB alterations occur in the majority of glioblastomas and are inversely correlated. *Cancer Res* 1996;56:150–3.
- Solomon DA, Kim JS, Jenkins S, et al. Identification of p18INK4c as a tumor suppressor gene in glioblastoma multiforme. *Cancer Res* 2008;68:2564–9.
- Wiedemeyer R, Brennan C, Heffernan TP, et al. Feedback circuit among INK4 tumor suppressors constrains human glioblastoma development. *Cancer Cell* 2008;13:355–64.
- The Cancer Genome Atlas Network. Comprehensive genomic characterization defines human glioblastoma genes and core pathways. *Nature* 2008;455:1061–8.
- Parsons DW, Jones S, Zhang X, et al. An integrated genomic analysis of human glioblastoma multiforme. *Science* 2008;321:1807–12.
- Lapenna S, Giordano A. Cell cycle kinases as therapeutic targets for cancer. *Nat Rev Drug Discov* 2009;8:547–66.
- Toogood PL, Harvey PJ, Repine JT, et al. Discovery of a potent and selective inhibitor of cyclin-dependent kinase 4/6. *J Med Chem* 2005;48:2388–406.
- Fry DW, Harvey PJ, Keller PR, et al. Specific inhibition of cyclin-dependent kinase 4/6 by PD 0332991 and associated antitumor activity in human tumor xenografts. *Mol Cancer Ther* 2004;3:1427–38.
- Vaughn DJ, Flaherty K, Lal P, et al. Treatment of growing teratoma syndrome. *N Engl J Med* 2009;360:423–4.
- Baughn LB, Di Liberto M, Wu K, et al. A novel orally active small molecule potently induces G1 arrest in primary myeloma cells and prevents tumor growth by specific inhibition of cyclin-dependent kinase 4/6. *Cancer Res* 2006;66:7661–7.
- Zhang C, Yan Z, Arango ME, Painter CL, Anderes K. Advancing bioluminescence imaging technology for the evaluation of anticancer agents in the MDA-MB-435-HAL-Luc mammary fat pad and subrenal capsule tumor models. *Clin Cancer Res* 2009;15:238–46.
- Villano JL, Seery TE, Bressler LR. Temozolomide in malignant

- gliomas: current use and future targets. *Cancer Chemother Pharmacol* 2009;64:647–55.
18. Ishii N, Maier D, Merlo A, et al. Frequent co-alterations of TP53, p16/CDKN2A, p14ARF, PTEN tumor suppressor genes in human glioma cell lines. *Brain Pathol* 1999;9:469–79.
  19. Giannini C, Sarkaria JN, Saito A, et al. Patient tumor EGFR and PDGFRA gene amplifications retained in an invasive intracranial xenograft model of glioblastoma multiforme. *Neuro-oncol* 2005;7:164–76.
  20. Sarkaria JN, Yang L, Grogan PT, et al. Identification of molecular characteristics correlated with glioblastoma sensitivity to EGFR kinase inhibition through use of an intracranial xenograft test panel. *Mol Cancer Ther* 2007;6:1167–74.
  21. Solomon DA, Kim JS, Cronin JC, et al. Mutational inactivation of PTPRD in glioblastoma multiforme and malignant melanoma. *Cancer Res* 2008;68:10300–6.
  22. Solomon DA, Kim JS, Ransom HW, et al. Sample type bias in the analysis of cancer genomes. *Cancer Res* 2009;69:5630–3.
  23. Bigner SH, Humphrey PA, Wong AJ, et al. Characterization of the epidermal growth factor receptor in human glioma cell lines and xenografts. *Cancer Res* 1990;50:8017–22.
  24. Camphausen K, Purov B, Sproull M, et al. Influence of *in vivo* growth on human glioma cell line gene expression: convergent profiles under orthotopic conditions. *Proc Natl Acad Sci U S A* 2005;102:8287–92.
  25. Hodgson JG, Yeh RF, Ray A, et al. Comparative analyses of gene copy number and mRNA expression in glioblastoma multiforme tumors and xenografts. *Neuro-oncol* 2009;11:477–87.
  26. Chang JE, Khuntia D, Robins HI, Mehta MP. Radiotherapy and radiosensitizers in the treatment of glioblastoma multiforme. *Clin Adv Hematol Oncol* 2007;5:894–902, 907–15.
  27. Reardon DA, Dresemann G, Taillibert S, et al. Multicentre phase II studies evaluating imatinib plus hydroxyurea in patients with progressive glioblastoma. *Br J Cancer* 2009;101:1995–2004.
  28. Mellinghoff IK, Wang MY, Vivanco I, et al. Molecular determinants of the response of glioblastomas to EGFR kinase inhibitors. *N Engl J Med* 2005;353:2012–24.
  29. Alonso M, Tamasdan C, Miller DC, Newcomb EW. Flavopiridol induces apoptosis in glioma cell lines independent of retinoblastoma and p53 tumor suppressor pathway alterations by a caspase-independent pathway. *Mol Cancer Ther* 2003;2:139–50.
  30. Burns KL, Ueki K, Jhung SL, Koh J, Louis DN. Molecular genetic correlates of p16, cdk4, and pRb immunohistochemistry in glioblastomas. *J Neuropathol Exp Neurol* 1998;57:122–30.
  31. Menu E, Garcia J, Huang X, et al. A novel therapeutic combination using PD 0332991 and bortezomib: study in the 5T33MM myeloma model. *Cancer Res* 2008;68:5519–23.
  32. Finn RS, Dering J, Conklin D, et al. PD 0332991, a selective cyclin D kinase 4/6 inhibitor, preferentially inhibits proliferation of luminal estrogen receptor-positive human breast cancer cell lines *in vitro*. *Breast Cancer Res* 2009;11:R77.

## Supplemental Table and Figure Legends

**Table S1.** Genetic lesions of the major known GBM oncogenes and tumor suppressor genes in a panel of 21 GBM cell lines. These data are derived from exonic sequencing and Affymetrix 250K SNP arrays performed by Solomon et al. (Cancer Res 68:2564-9, 2008; Cancer Res 68:10300-6, 2008; Cancer Res 69:5630-3, 2009), TP53 sequencing from Van Meir et al. (Cancer Res 54:649-52, 1994), Affymetrix 6.0 SNP arrays performed by the Cancer Genome Project of the Wellcome Trust Sanger Institute (<http://www.sanger.ac.uk/genetics/CGP/>), and from the COSMIC database also of the Cancer Genome Project. \*, mutation status of gene not determined.

**Figure S1.** Western blots for the major known GBM oncogenes and tumor suppressor genes on a panel of 21 GBM cell lines. Genetic lesions of the cdk4/6-cyclin D-INK4-Rb signaling pathway present in these 21 cell lines detailed in Supplemental Table 1 that result in altered gene expression can be seen. 15/21 of these cell lines have homozygous deletion of CDKN2A/B and make no detectable p16<sup>INK4a</sup> protein, 5/21 have homozygous deletion or mutation of RB1 that result in no detectable Rb protein, 4/21 have homozygous deletion of CDKN2C that results in no detectable p18<sup>INK4c</sup> protein, and 1/21 has amplifications of both CDK6 and CCND3 that result in significant overexpression of cdk6 and cyclin D3 proteins. Lesions of CDKN2A/B, RB1, and CDK6/CCND3 are mutually exclusive in these 21 cell lines, except in 42MGBA cells which harbor homozygous deletion of CDKN2A/B and are also Rb-deficient. In contrast, homozygous deletions of CDKN2C are not mutually exclusive with CDKN2A/B, RB1, and CDK6/CCND3 lesions, and in fact are present exclusively in cells with homozygous deletions of CDKN2A/B. A number of additional genetic lesions in other signaling pathways detailed in Supplemental Table 1 that result in altered gene expression in these cells can also be seen. 11/21 of these cell lines have homozygous deletion or mutation of PTEN resulting in scant or absent protein levels, 2/21 have EGFR rearrangement resulting in EGFR protein at aberrant molecular weights, and 2/21

have MDM2 amplification resulting in significant overexpression of Mdm2 protein. No significant concordance was detected between any of these other genetic lesions and lesions of cdk4/6-cyclin D-INK4-Rb signaling pathway genes.

**Figure S2.** PD-0332991 induces cell cycle arrest of GBM cells dependent on Rb status. A panel of 21 GBM cell lines was cultured *in vitro* in the presence of vehicle or 1  $\mu$ M PD-0332991 for 48 hrs, pulsed with BrdU for 1 hr, then fixed and stained with propidium iodide and FITC-conjugated BrdU antibody for flow cytometry analysis. Cell cycle distribution plots of BrdU vs. propidium iodide (PI) intensity are shown.

**Figure S3.** Dose response of GBM cell lines with partial or no response to 1  $\mu$ M PD-0332991. The panel of 21 GBM cell lines was cultured *in vitro* in the presence of 0, 1, 2, or 10  $\mu$ M PD-0332991, and cell cycle distribution was assessed at 48 hrs post-treatment by staining with propidium iodide and FITC-conjugated BrdU antibody following a 1 hr BrdU pulse before fixation. Cell lines with homozygous lesions of RB1 (*e.g.* 8MGBA, GMS10, and LN405) displayed no significant reduction in BrdU incorporation or other alteration in cell cycle distribution at any of the doses tested. Of the Rb-proficient cells, those that displayed a 10-95% reduction in BrdU incorporation at a dose of 1  $\mu$ M PD-0332991 (*e.g.* AM38, Hs683, T98G, GAMG, and LN18) demonstrated increased reductions at doses of 2 and 10  $\mu$ M. Cells that displayed >95% reduction in BrdU incorporation at 1  $\mu$ M PD-0332991 demonstrated similar responses at doses of 2 and 10  $\mu$ M, and no evidence of cytotoxicity/apoptosis was apparent (*e.g.* sub-G1 DNA content) at any dose tested (data not shown).

**Table S2.** Mean survival data and statistical comparisons from the Kaplan-Meier survival plots in Fig. 3A *right panel*, Fig. 3D *right panel*, Fig. 4B, and Fig. 5C. Statistically significant comparisons ( $p < 0.05$ ) are highlighted in bold.

**Figure S4.** PD-0332991 fails to suppress the growth of intracranial xenografts generated from an Rb-deficient cell line SF767. Bioluminescence monitoring of mice bearing intracranial xenografts generated from Rb-proficient U87MG cells and Rb-deficient SF767 cells during treatment with vehicle (Control) or PD-0332991 (150 mg/kg/day from day 13-27).

## Supplemental Table 1

cell line	RB signaling								Genetic
	RB1	CDKN2A/B	CDKN2C	CDK4*	CDK6*	CCND1*	CCND2*	CCND3*	p53 signal TP53
8MGBA	homozygous deletion								homozygous missense
42MGBA	no protein expression*	homozygous deletion							*
A172		homozygous deletion							
AM-38		homozygous deletion							
CCF-STTG1		hemizygous deletion			amplified			amplified	
DBTRG-05MG		homozygous deletion							
DKMG		homozygous deletion							
GAMG		homozygous deletion							homozygous missense
GMS10	homozygous nonsense								homozygous missense
H4		homozygous deletion							
Hs683	*	homozygous deletion							*
KG-1-C	*	homozygous deletion							*
LN18	*	homozygous deletion							heterozygous missense
LN229	*	homozygous deletion	homozygous deletion						heterozygous missense
LN405	homozygous nonsense								homozygous missense
M059J	homozygous splice site								
NMC-G1		homozygous deletion							
SNB19		homozygous deletion	homozygous deletion						homozygous missense
T98G		homozygous deletion	homozygous deletion						homozygous missense
U138MG		homozygous deletion							homozygous missense
U87MG		homozygous deletion	homozygous deletion						
<b>Total events</b>	<b>5</b>	<b>17</b>	<b>4</b>	<b>0</b>	<b>1</b>	<b>0</b>	<b>0</b>	<b>1</b>	<b>9</b>
<b>Frequency</b>	<b>24%</b>	<b>81%</b>	<b>19%</b>	<b>0%</b>	<b>5%</b>	<b>0%</b>	<b>0%</b>	<b>5%</b>	<b>43%</b>

lesions present in cells							
ling		Receptor tyrosine kinase signaling			PI3-Kinase signaling		additional pathways
MDM2*	MDM4*	EGFR	PDGFRA	BRAF	PIK3CA	PTEN	other
		*	*		*	no protein expression*	
		focal gain, rearranged			focal gain	homozygous deletion	
amplified				homozygous mutation		homozygous missense	
				heterozygous mutation		homozygous deletion	
amplified		amplified, rearranged			heterozygous mutation		
							SMAD4, homozygous deletion
						hemizygous deletion	NF1, homozygous deletion
						homozygous deletion	
		*	*		*		
		*	*	heterozygous mutation	*	*	
		*	*		*		
		*	*		*		
						homozygous missense	
						homozygous frameshift	
				heterozygous mutation			NF2, homozygous frameshift
			focal gain			homozygous frameshift	NOTCH2, amplified
						homozygous missense	TCF7L2, homozygous deletion
						homozygous splice site	
						homozygous splice site	
2	0	2	1	4	2	12	5
10%	0%	10%	5%	19%	10%	57%	24%

Figure S1

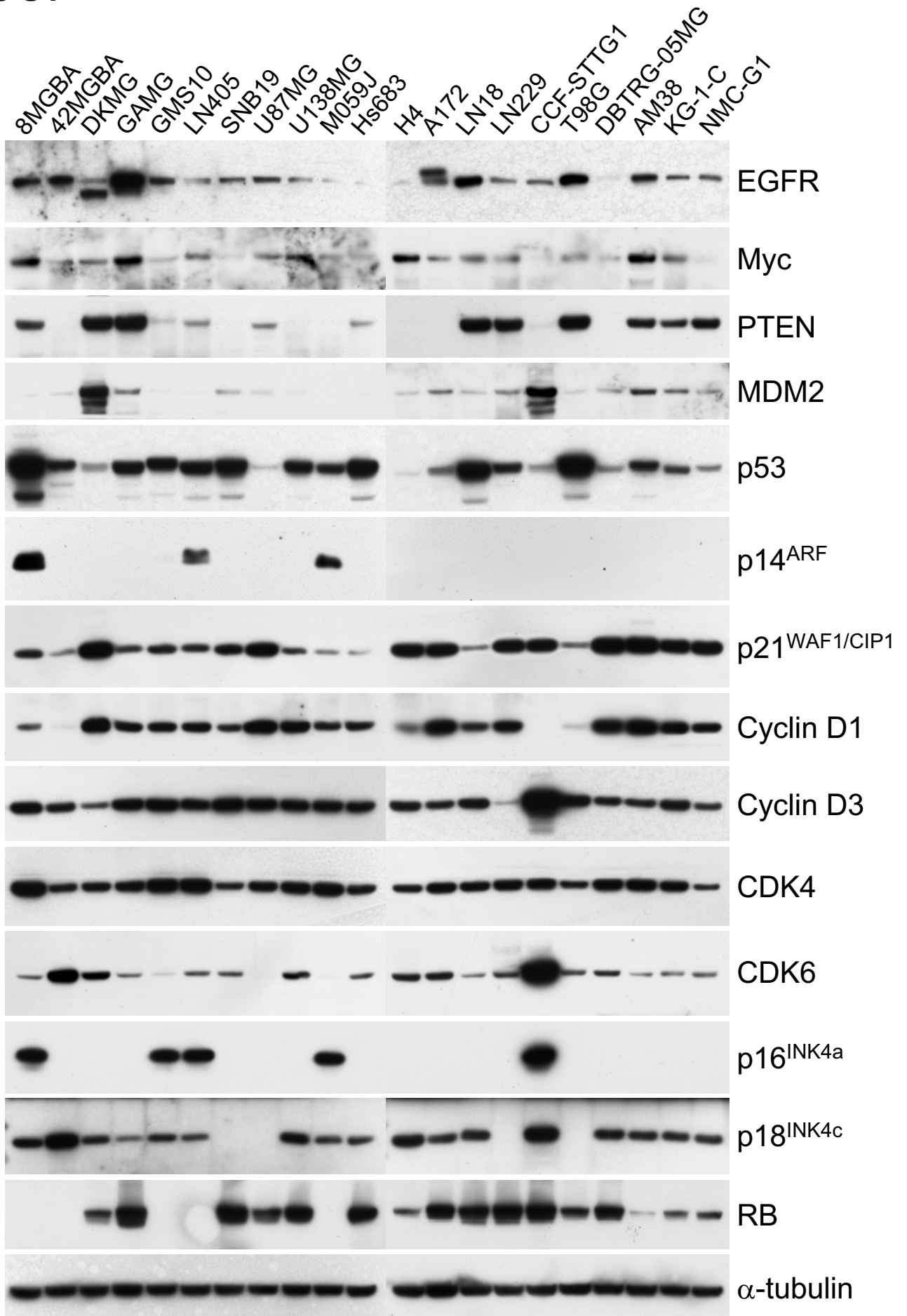
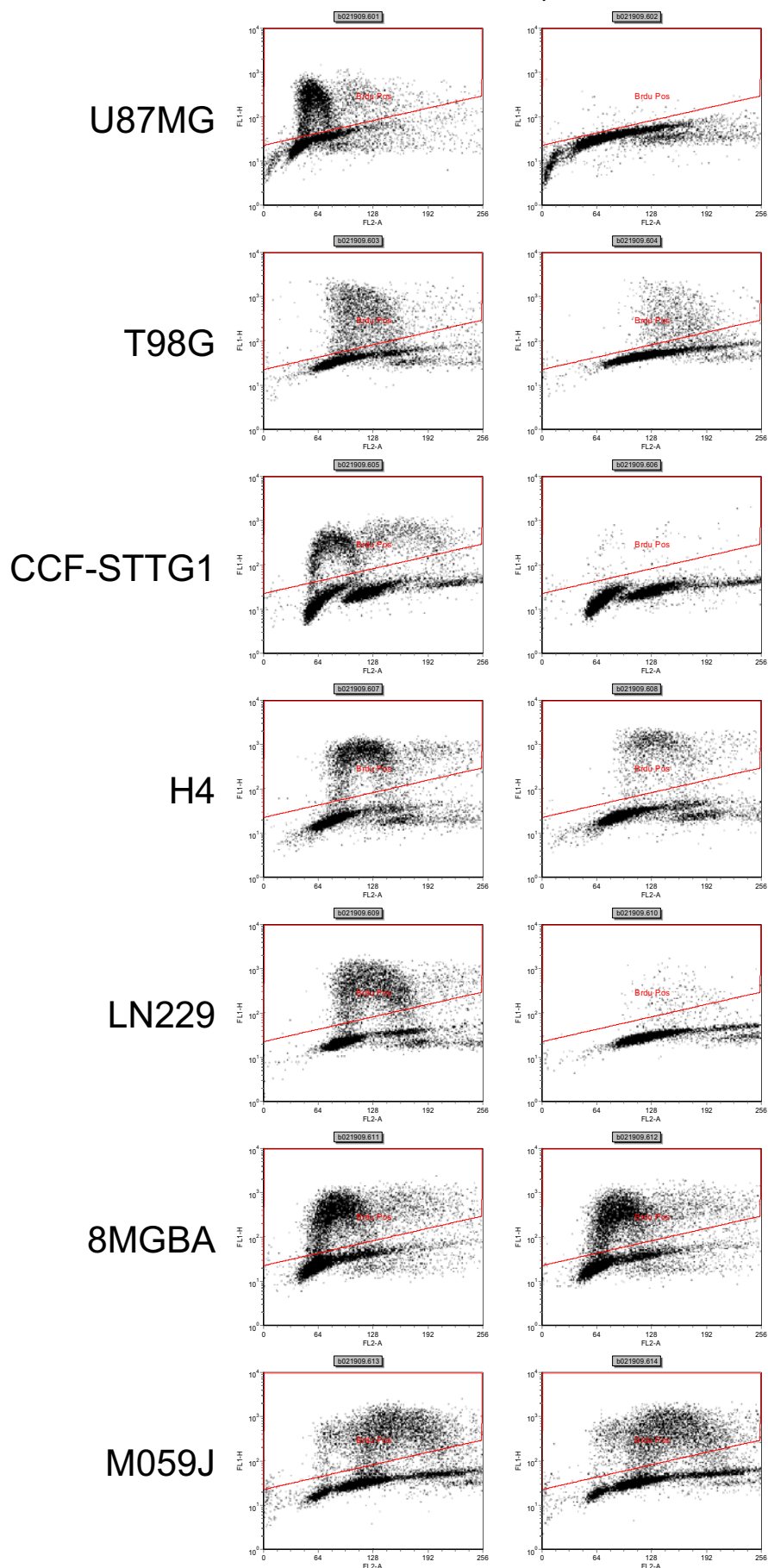


Figure S2

+ vehicle + 1  $\mu$ M PD-0332991



# Figure S2 continued

+ vehicle + 1  $\mu$ M PD-0332991

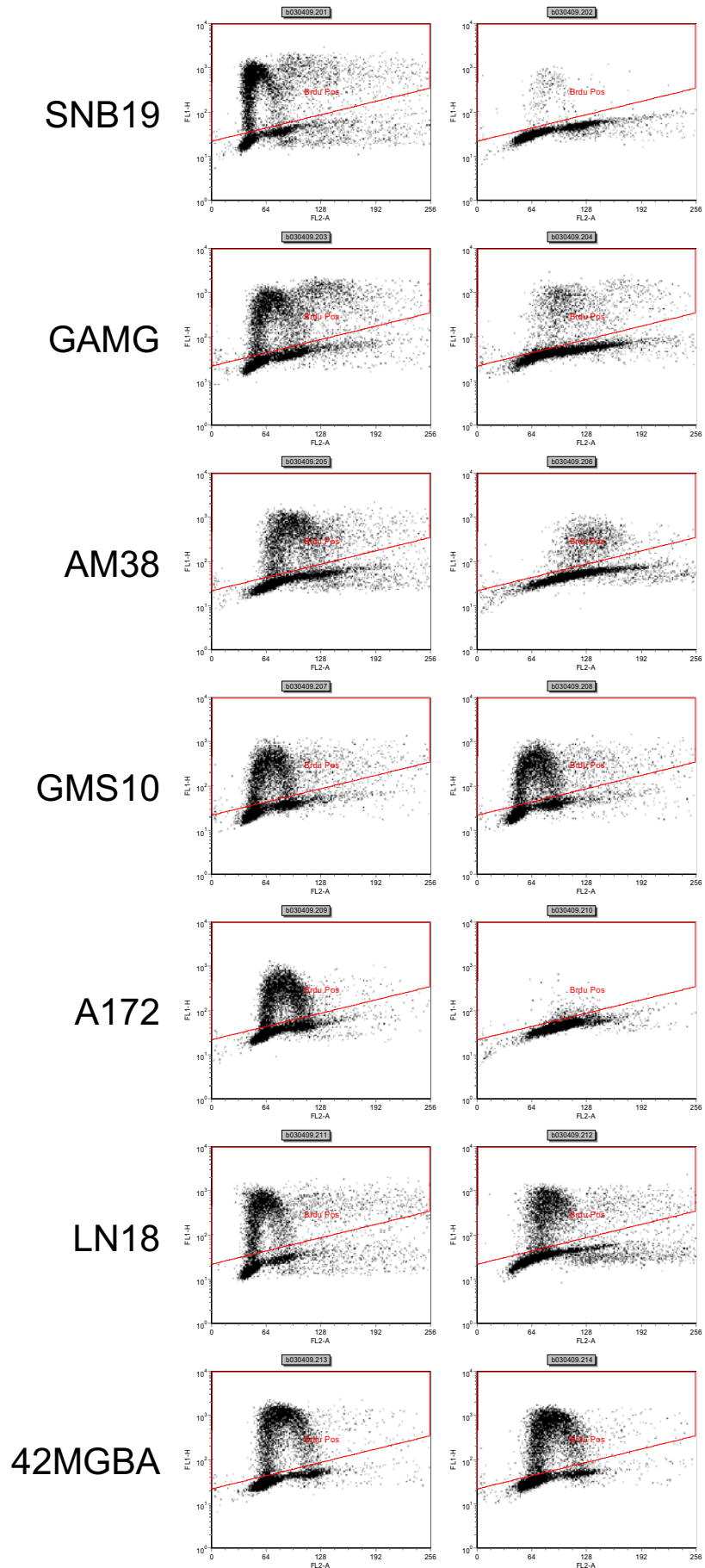


# Figure S2 continued

+ vehicle + 1  $\mu$ M PD-0332991

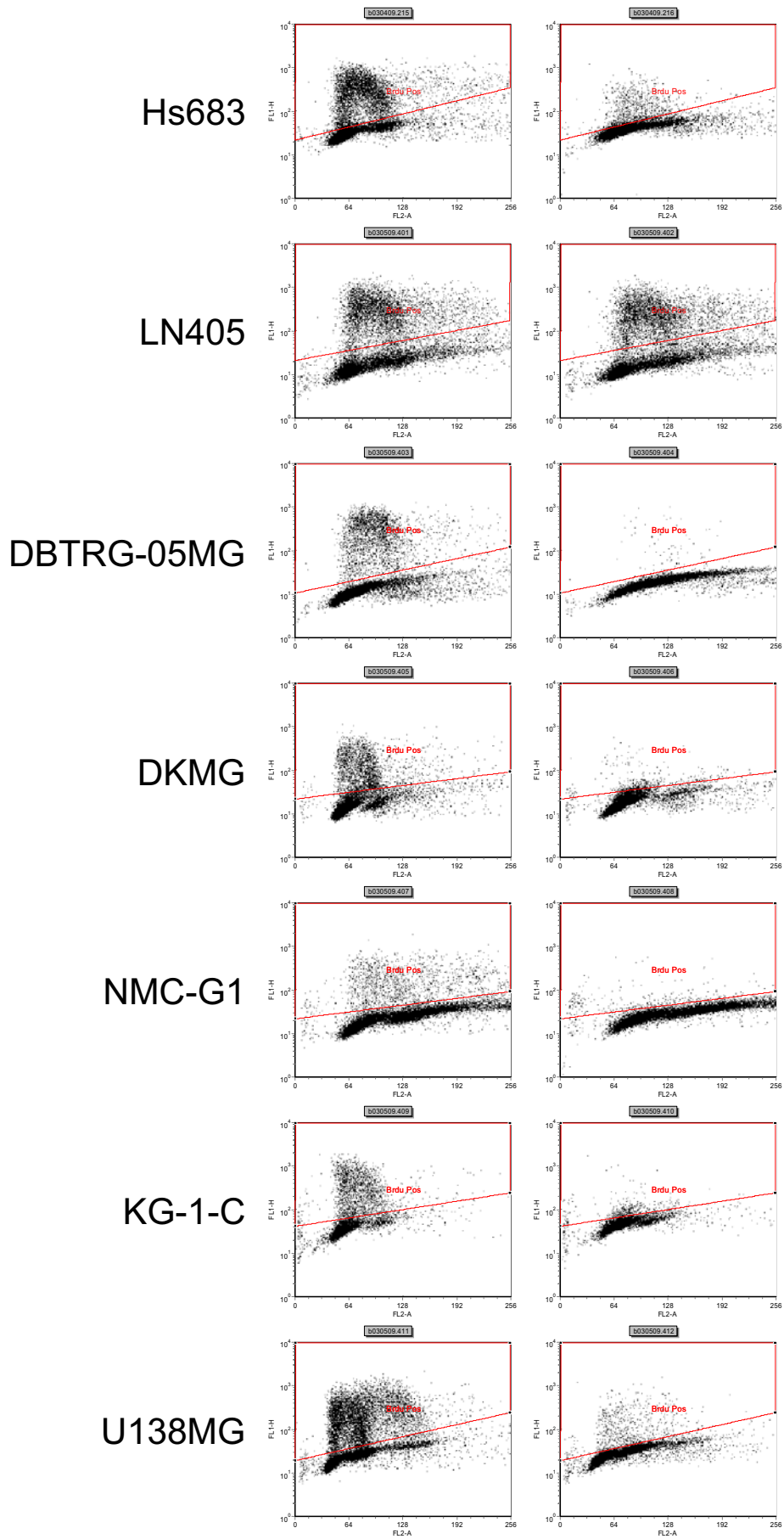
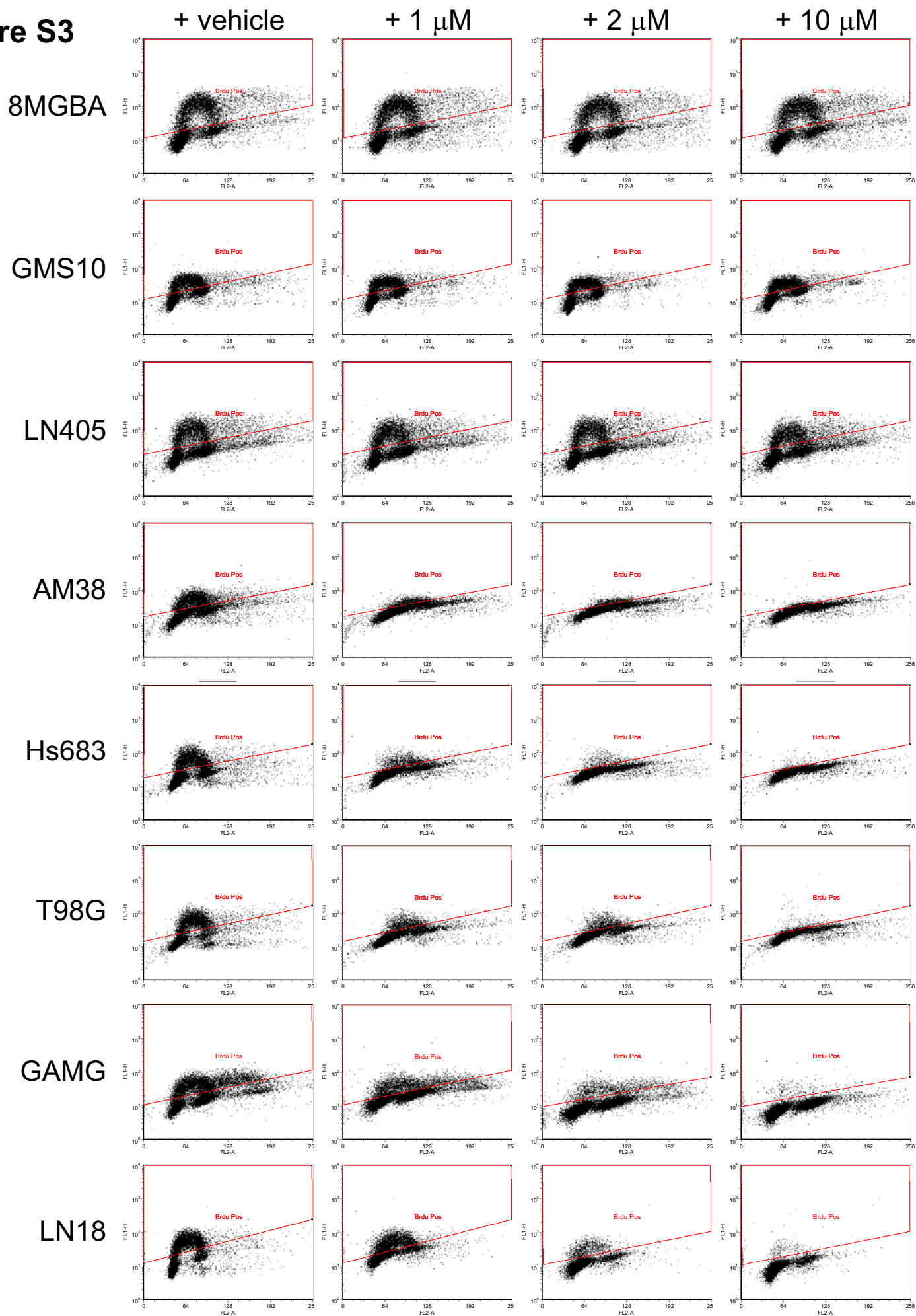


**Figure S3**



## Supplemental Table 2

### **U87MG + PD-0332991 Monotherapy (Fig. 3A)**

Group	Mean survival	Survival comparison
Control	34.2 days	<b>p &lt; 0.001</b>
PD-0332991	>58.6 days	

### **GBM 39 + PD-0332991 Monotherapy (Fig. 3D)**

Group	Mean survival	Survival comparison
Control	85.4 days	<b>p &lt; 0.001</b>
PD-0332991	>122 days	

### **U87MG + PD-0332991 + Radiation Combination Therapy (Fig. 4B)**

Group	Mean survival	Survival comparisons
Control	29.0 days	<b>p &lt; 0.001 (all comparisons)</b>
PD-0332991 only	46.6 days	p = 0.900 (RT only) p = 0.072 (PD-0332991 + RTc) <b>p = 0.010 (PD-0332991 + RTs)</b>
RT only	44.0 days	<b>p = 0.038 (PD-0332991 + RTc)</b> <b>p = 0.011 (PD-0332991 + RTs)</b>
PD-0332991 + RTc	51.1 days	p = 0.181 (PD-0332991 + RTs)
PD-0332991 + RTs	51.4 days	

### **U87MG Recurrent Tumors + PD-0332991 (Fig. 5C)**

Group	Mean survival	Survival comparisons
No treatment	56.5 days	<b>p = 0.005 (TMZ only)</b> <b>p = 0.007 (PD-0332991 only)</b> <b>p &lt; 0.001 (TMZ + PD-0332991)</b>
PD-0332991 only	73.3 days	p = 0.383 (TMZ only) p = 0.155 (TMZ + PD-0332991)
TMZ only	>78.1 days	p = 0.970 (TMZ + PD-0332991)
PD-0332991 + TMZ	>81.4 days	

Figure S4

